

# Remote laser detection of natural gas leakages from pipelines

V.O. Petukhov, V.A. Gorobets, Yu.M. Andreev, G.V. Lanskii

**Abstract.** A differential absorption lidar based on a tunable TEA CO<sub>2</sub> laser emitting at 42 lines of the ‘hot’ 01<sup>1</sup>1–11<sup>1</sup>0 band in the range from 10.9 to 11.4 μm is developed for detecting natural gas leakages from oil pipelines by measuring the ethane content in the atmosphere. The ethane detection sensitivity is 0.9 ppm km. The presence of methane does not distort the measurement results. The developed lidar can detect the natural gas leakage from kilometre heights at the flying velocities up to 200 km h<sup>-1</sup> and a probe pulse repetition rate of 5 Hz.

**Keywords:** CO<sub>2</sub> laser, natural gas, probing, leakages.

## 1. Introduction

It is assumed that at present the annual total volume of the natural gas leakage during its extraction, transport and usage is 10<sup>8</sup> m<sup>3</sup>. Such losses have not only large material tolls but also have a severe impact on the population and can cause the change in climate due to the greenhouse effect. The remote detection of leakage sites in pipelines can be performed by a number of methods, including the most sensitive and rapid differential optical absorption method [1]. As follows from the natural gas composition (Table 1), the detection of leakage sites by measuring the excess concentration of methane in the atmosphere looks attractive due its high content.

Among the absorption bands of the main isotope <sup>12</sup>CH<sub>4</sub> of methane at 12.8, 7.7, 3.3, 2.3, 1.66, 1.57, 1.34, and 0.77 μm, the intense 3.3-μm absorption band in the mid-IR range attracts the greatest attention in the development of various differential absorption lidars. This is also facilitated by the fact that many lasers emitting within this band are available, unlike the most intense 7.7-μm absorption band,

**Table 1.** Gas composition in deposits in the Eastern Siberia [2].

Deposit	Main components (mass %)				
	CH <sub>4</sub>	C <sub>2</sub> H <sub>6</sub>	C <sub>3</sub> H <sub>8</sub> , C <sub>4</sub> H <sub>10</sub> , C <sub>5</sub> H <sub>12</sub> , C <sub>6</sub> H <sub>14</sub>	N <sub>2</sub>	He
Kovyktinskoe	91.39	4.91	1.78	1.52	0.28
Chayandinskoe	85.48	4.57	2.58	6.44	0.5
Yurbcheno- Tokhomscoe	81.11	7.31	5.06	6.39	0.18
Sredne- botuobinskoe	88.61	4.95	3.12	2.93	0.2–0.6

which is strongly overlapped by the tail of the fundamental absorption band of water vapour.

The development of the most demanded remote lidars operating in the 3-μm region is a complicated technical problem for a number of reasons. In fact, this is the region of not one isolated but several overlapped absorption bands of methane lying in the spectral ranges 3.07–3.43, 3.17–3.47, 3.12–3.56, 3.16–3.89, and 3.15–3.75 μm containing 6508 narrow ( $\Delta\nu \sim 0.01$  cm<sup>-1</sup>) absorption lines of intensity from 10<sup>-24</sup> to 2.1 × 10<sup>-19</sup> cm mol<sup>-1</sup>. The intense vibrational–rotational absorption bands of many organic gases related to the C–H bond and the absorption bands of water vapour are also located in this region. The measurement results considerably depend on the high (1.7 ppm) background content of methane upon the large emission of natural and agricultural methane. Because the molecular weight of methane is smaller than that of air, methane is not accumulated in leakage sites. Finally, high-power narrow-band tunable lasers with high pulse repetition rates and reliability emitting in the 3.3-μm region are not commercially available.

The parameters of available tunable diode lasers allow path measurements and the remote detection of methane with the extremely low signal-to-noise ratio [3–6] by using topographic objects as reflectors located at a distance of no more than 1 km. The emission spectra of these lasers are complex and strongly depend on temperature, while laser beams have the multimode structure. Difference-frequency oscillators converting the radiation frequency of high-power visible and near-IR lasers to the mid-IR range have the low efficiency because of the absence of nonlinear crystals with acceptable optical linear and nonlinear properties [7]. For this reason, the typical output energy parameters of frequency-converted radiation are close to those of semiconductor lasers. This also concerns parametric narrowband

V.O. Petukhov, V.A. Gorobets B.I. Stepanov Institute of Physics, National Academy of Sciences of Belarus, prosp. Nezavisimosti 68, 220072 Minsk, Belarus; e-mail: v.petukhov@ifanbel.bas-et.by, v.gorobets@ifanbel.bas-net.by;

Yu.M. Andreev, G.V. Lanskii Institute of Monitoring of Climatic and Ecological Systems, Siberian Division, Russian Academy of Sciences, prosp. Akademicheskii 10/3, 634055 Tomsk, Russia; e-mail: yuandreev@imces.ru, lanskyy@yandex.ru

Received 11 November 2009

Kvantovaya Elektronika 40 (2) 173–177 (2010)

Translated by M.N. Sapozhnikov

tunable mid-IR oscillators, which can operate reliably only at output pulse energies of no more than a few tens of millijoules at pulse repetition rates up to a few tens of hertz [8–11].

The application of chemical lasers and TEA CO<sub>2</sub> lasers generating the third harmonic or the sum frequency of fundamental radiation and second harmonic is hampered by accident coincidences of radiation lines with weak absorption lines, the low output energy parameters of CO<sub>2</sub> lasers and by complicated handling of chemical and CO<sub>2</sub> lasers. Thus, because of a low absorption cross section, the methane detection sensitivity in measurements at the P<sub>1</sub>(9) line of a DF laser is 6 ppm km [12]. The application of the third harmonic of CO<sub>2</sub> lasers emitting at the 10R(20), 10R(18), 9P(20), and 9P(18) lines is not promising because of a low absorption cross section ( $\sigma = 1.8$  and  $1.7 \text{ cm}^{-1} \text{ atm}^{-1}$ ) and poor coincidence (0.1699 and  $0.069 \text{ cm}^{-1}$ , respectively) with absorption line maxima [13]. The possibility of measurements at a wavelength of  $3.3922 \text{ }\mu\text{m}$  emitted by a He–Ne laser, which coincides with the P(7) absorption line of methane, is limited by a low output power and the interference by the absorption lines of water vapour. The low absorption cross section restricts the application of a Co : MgF<sub>2</sub> laser emitting in the region from  $1.5$  to  $3.2 \text{ }\mu\text{m}$  [14].

The low absorption cross sections at shorter-wavelength absorption bands, for example,  $\sigma = 0.59 \text{ cm}^{-1} \text{ atm}^{-1}$  at a wavelength of  $1.6449 \text{ }\mu\text{m}$  emitted by a Er<sup>3+</sup> : YAG laser [15], also restrict the use of this laser. As a result, remote lidars for detecting the leakage sites of natural gas by measuring the methane content in the atmosphere have low parameters and should be mounted in slowly flying helicopters at small heights, which blow the gas away from the leakage site (Table 2).

In this paper, we developed a TEA CO<sub>2</sub> laser emitting 0.5–2-J pulses, which can be tuned over the lines in the hot 01<sup>1</sup>1–11<sup>1</sup>0 band, and built a differential absorption CO<sub>2</sub> laser lidar for detecting the leakage sites of natural gas from pipelines by measuring the ethane content in the atmosphere.

## 2. CO<sub>2</sub> laser

The TEA CO<sub>2</sub> lasers used for remote lidar gas analysis should have the high output power, the improved mode structure of the output beam, the low divergence and narrow width of the line located near the maximum of the amplification band and absorption band of the gas. Having studied in detail the conditions providing efficient lasing at the unconventional lines of CO<sub>2</sub> lasers [17, 18], we developed a small ( $100 \times 35 \times 40\text{-cm}$ , 50 kg) and reliable TEA CO<sub>2</sub> laser, which can be automatically tuned over discrete emission wavelengths in a broad range.

The laser resonator of length  $\sim 1 \text{ m}$  is formed by a diffraction grating ( $100$  or  $150 \text{ lines mm}^{-1}$ , the reflectance to

the first order is no less than 95 %) and a plane dichroic mirror with the reflectance  $\sim 85 \%$  through which radiation was coupled out. An important feature of the laser is the specific composition of the active medium (CO<sub>2</sub> : N<sub>2</sub> : He = 35 : 30 : 35) at the total relatively low pressure 200–250 Torr, which considerably differs from the composition of typical active media of TEA CO<sub>2</sub> lasers (CO<sub>2</sub> : N<sub>2</sub> : He = 20 : 20 : 60,  $P = 760 \text{ Torr}$ ) emitting in the region of fundamental bands. The main discharge with the UV preionisation is ignited between profiled electrodes of length 70 cm and width 2.5 cm. The interelectrode gap is 2 cm. The 0.2- $\mu\text{F}$  storage capacitor is charged up to 20 kV. A specially developed low-inductance ( $\sim 50 \text{ nH}$ ) power supply of the laser provides a stable glow discharge in a broad pressure range and a broad range of active-medium compositions at high energy supplies (up to  $1000 \text{ J L}^{-1} \text{ atm}^{-1}$ ).

This power supply and active-medium composition provide the maximum lasing efficiency at the lines of the hot 01<sup>1</sup>1–11<sup>1</sup>0 emission band. In this case, the lasing efficiency at the fundamental and sequence emission bands decreases only slightly. During operation in the repetitively pulsed regime with a pulse repetition rate of up to 5 Hz without the circulation of the active medium, the reproducibility of the output parameters of the laser is virtually the same as for active media of the traditional composition.

The description of other design features of the developed laser is presented in [17, 18]. As a whole, the laser emits more than 200 lines in the fundamental (00<sup>0</sup>1–10<sup>0</sup>0, 02<sup>0</sup>0), second sequence (00<sup>0</sup>2–10<sup>0</sup>1, 02<sup>0</sup>1) and hot (01<sup>1</sup>1–11<sup>1</sup>0) bands.

The laser can emit 42 lines in the hot 01<sup>1</sup>1–11<sup>1</sup>0 band between 10.9 and 11.4  $\mu\text{m}$ , from the P(12) to P(53) line with the single pulse energy  $E_{\text{out}} \geq 0.5 \text{ J}$ . The laser pulse energy in the range 11.2–11.3  $\mu\text{m}$  is 1.0–1.5 J, and it achieves 2 J at the most intense lines in the range 11.0–11.2  $\mu\text{m}$ . The duration of the main laser peak containing 60 % of the total pulse energy is 200–250 ns, while the total pulse duration with the nitrogen emission ‘tail’ achieves 2  $\mu\text{s}$ . The peak power of the most intense emission lines exceeds 5 MW. By using two apertures of diameter 20 mm, which are located in front of the diffraction grating and output mirror, we obtained the optimal relation between the energy and spectral parameters of the laser. In this case, the laser spot of diameter  $\sim 20 \text{ mm}$  acquires a nearly circular shape and homogeneous spatial structure. The radiation divergence at the hot-band lines is 1–1.5 mrad and the linewidth is  $\sim 0.01 \text{ cm}^{-1}$ .

The wavelengths of all the emission lines is well known, they are well separated ( $0.5\text{--}2 \text{ cm}^{-1}$ ) and, hence, can be easily spectrally selected by using a computer-controlled step motor. Note that the number of lines in the hot band is twice that in the case of usual transitions due to the presence of even and odd transitions.

**Table 2.** Parameters of domestic lidar systems for detecting natural-gas leakage sites in pipelines by measuring the methane content in the atmosphere [16].

Lidar system	Flying speed/km h <sup>-1</sup>	Flying height/m	Detection sensitivity/ppm km	Consumed power/kW	Mass/kg	Response time/s
Obzor-2	60–120	30–70	0.9	1	250	0.15
MAG-1	60–120	30–100	0.9	0.3	60	0.1–0.3
Aeropoisk	80–120	30–80	–	0.3	40	–

### 3. Model estimates

The model absorption spectra of  $\text{CH}_4$ ,  $\text{C}_2\text{H}_6$  and the bottom layer of the atmosphere (summer middle latitude model, the total pressure  $P = 1$  atm,  $T = 296$  K, the  $\text{H}_2\text{O}$  vapour concentration is 7750 ppm) for a measurement path length of 200 m calculated by using the HITRAN 2004 data base are presented in Fig. 1.

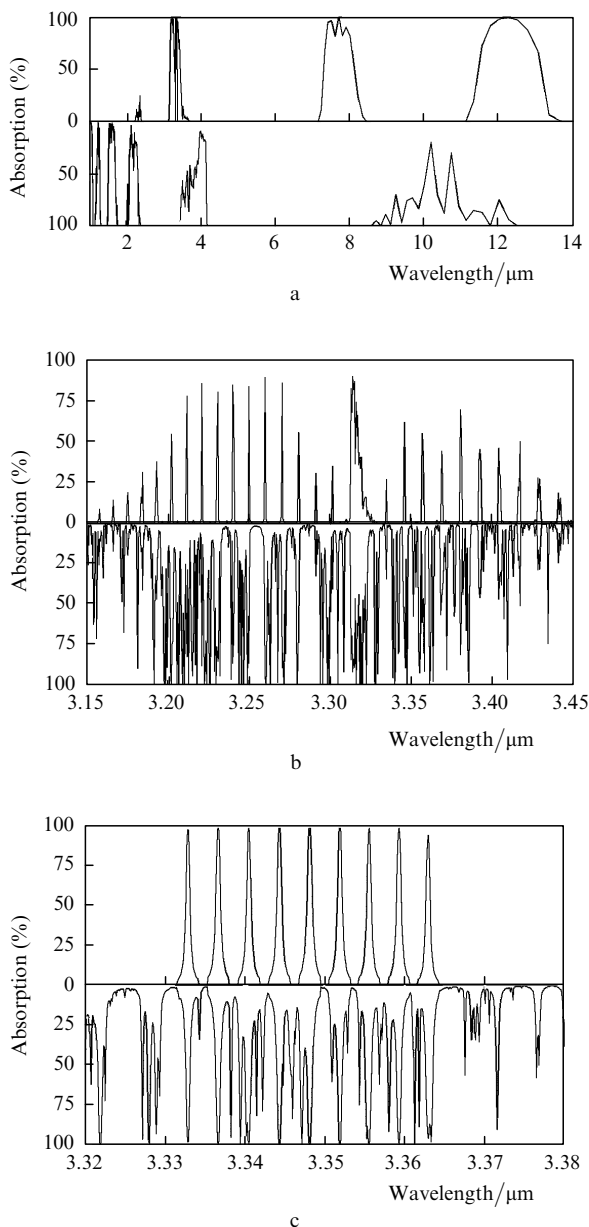


**Figure 1.** Model absorption spectra of 1.7 ppm  $\text{CH}_4$  and 10 ppm  $\text{C}_2\text{H}_6$  (upper part of the figure) and of the bottom layer of the atmosphere (lower part of the figure) recorded with a spectral resolution of  $2\text{ cm}^{-1}$  (a), and of  $\text{CH}_4$  and atmosphere (b) and  $\text{C}_2\text{H}_6$  and atmosphere (c) recorded with a spectral resolution of  $0.05\text{ cm}^{-1}$  (upper and lower parts of the figure, respectively).

Figure 1 shows that ethane has isolated absorption lines in the 3.3- $\mu\text{m}$  region, for example, in the transparency windows 3.332–3.334  $\mu\text{m}$  and 3.335–3.338  $\mu\text{m}$ , as methane in the region from 3.3125 to 3.3145  $\mu\text{m}$ . The width of the absorption lines of ethane is several times larger and they

are better distinguished. However, it is obvious that the measurement of the ethane content by absorption spectra in the 3- $\mu\text{m}$  region should be complicated by the same factors as that of methane.

The short-wavelength part of the absorption band in the 12- $\mu\text{m}$  region lies near the transparency windows of the atmosphere and coincides with the hot  $01^11-11^10$  emission band of  $\text{CO}_2$  lasers. For the model atmosphere used in calculations in Fig. 1, by neglecting weak gas components of the atmosphere, the mutual arrangement of the absorption lines of methane, water vapour and the  $\text{CO}_2$  laser lines looks as shown in Fig. 2.

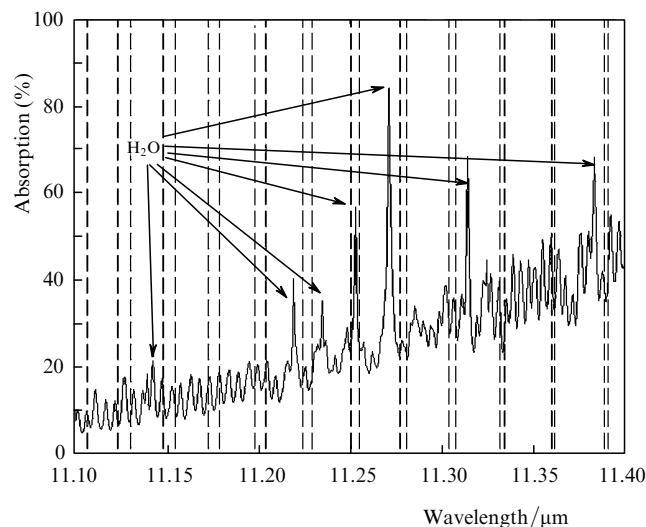


**Figure 2.** Model absorption spectrum of 10 ppm  $\text{C}_2\text{H}_6$  in a path of length 200 m. The dashed straight lines indicate the emission wavelengths of the  $\text{CO}_2$  laser in the hot  $01^11-11^10$  band, the arrows show the absorption lines of water vapour.

The spectral width of the absorption lines of ethane here is also several times larger than that of methane in the 3.3- $\mu\text{m}$  region and does not exceed the  $\text{CO}_2$  laser linewidth. The absorption spectra of most abundant organic gases in the 12- $\mu\text{m}$  region are well separated, while absorption in the atmospheric aerosol and inclusions is minimal, which is favourable for remote lidars, in which topographic objects are used as reflectors.

The possibility of measuring the ethane content in the atmosphere was calculated by the method presented in [19, 20]. The P(31) emission line at 11.1069  $\mu\text{m}$  ( $900.3383\text{ cm}^{-1}$ ) was used as a reference line, while the P(39) line at 11.2040  $\mu\text{m}$  ( $892.5395\text{ cm}^{-1}$ ) and P(50) line at 11.3601 ( $880.2739\text{ cm}^{-1}$ ) were used as on-line lines. In this case, the differential absorption cross section is 0.12 and  $0.23\text{ cm}^{-1}\text{ atm}^{-1}$ , respectively, and the detection sensitivity is about 0.9 ppm km. The distance between the selected pairs of lines is close to the admissible interval 5–10  $\text{cm}^{-1}$  excluding the influence of selective aerosol absorption on the results of measurements. It is also important that the selected pairs of laser lines are well separated from the absorption lines of water vapour and, therefore, measurements can be easily performed even in highly humid atmosphere.

## 4. Experiment

The developed TEA CO<sub>2</sub> laser was used in lidars (see Chapters 4 and 5 in monograph [20]) operating in measurement paths of length up to 8 and 12 km. In the second case, radiation was detected with a homemade cooled KRT photoresistor ( $\varnothing 1$  mm) with the time constant  $\sim 10$  ns and detection sensitivity  $2 \times 10^{10}$  cm Hz<sup>1/2</sup> W<sup>-1</sup>. In the reference channel a Vigo System S.A. PCI-L-3 pyroelectric detector (Poland) operating in the 2–12- $\mu$ m range with the response time less than 1 ns was used. The pulse shape was recorded with a two-channel 500-MHz TDS3052 (Tektronix, Inc.) oscilloscope. The reference and useful signals were measured with a peak detector.

It was found in tests performed under various weather conditions that the reflectance of topographic objects was in the range from a few percent for buildings and plywood sheets down to a few tenths–hundredths of percent for hill sides covered with grass. For  $\sim 1$ -J single probe pulses, the signal-to-noise ratio at the detector output exceeded  $10^4$  during dry weather. The efficiency of all systems of the lidar was preliminarily tested by detecting low (background) concentrations of NH<sub>3</sub>, O<sub>3</sub>, C<sub>2</sub>H<sub>4</sub>, CO, and H<sub>2</sub>O vapour under real field conditions in Minsk city (Belarus) at the wavelengths of the fundamental emission band and its second harmonic and comparing the results with earlier data. The possibility of detecting ethane was estimated by simulating the natural gas leakage by letting the gas into atmosphere directly in the measurement path. The system was calibrated and its sensitivity was determined by using a polyvinyl chloride cell of size  $0.5 \times 0.5 \times 2$  m with 100- $\mu$ m-thick polyethylene film windows filled with the known amount of ethane. The time dependence of the ethane amount in the atmosphere after its letting into the measurement path is shown in Fig. 3. The plot was constructed by using the smoothing procedure.

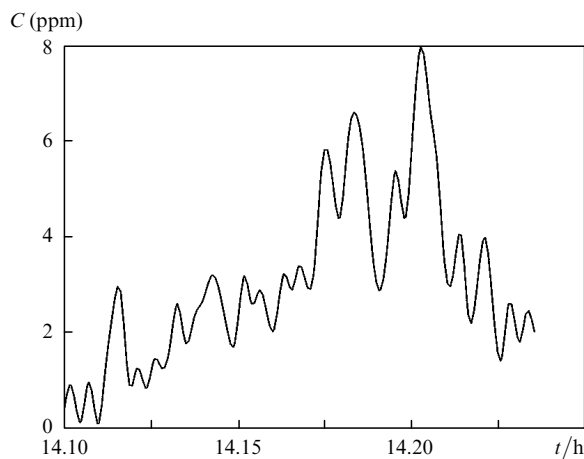


**Figure 3.** Time dependence of the ethane content in the bottom layer of the atmosphere path of length 200 m.

The calibration of the system showed that estimates were in good agreement with the experimental measurement sensitivity of 0.9 ppm km. The estimates showed that a hemispherical ethane cloud ( $\varnothing 30$  m) in the atmosphere can be detected when it contains 0.1 % of ethane. The advantage of ethane as an indicator of leakage sites is its low

background content (2 ppm) in the atmosphere, the low emission level of natural and anthropogenic sources and accumulation in the leakage sites because its molecular weight is greater than that of air. By using the laser with output energy parameters presented above, it is possible to detect ethane from kilometre heights at the flying velocity up to 200 km h<sup>-1</sup> and a pulse repetition rate of 5 Hz and the probe beam divergence  $5-10^\circ$ .

## 5. Conclusions

We have developed a small TEA CO<sub>2</sub> laser emitting more than 200 lines in the (00<sup>0</sup>1–10<sup>0</sup>0, 02<sup>0</sup>0) fundamental, second sequence (00<sup>0</sup>2–10<sup>0</sup>1, 02<sup>0</sup>1) and hot (01<sup>1</sup>1–11<sup>1</sup>0) emission bands. In the hot band the laser can emit 42 lines in the range from 10.9 to 11.4  $\mu$ m, from the P(12) to P(53) line with the output single pulse energy of 05–2 J, with the same reproducibility as during lasing in the fundamental bands. The laser has been tested in a remote differential absorption lidar used for detecting natural gas leakages by the excess content of ethane in the atmosphere employing topographic objects as reflectors. The ethane detection sensitivity was 0.9 ppm km. To build lidars based on this method, it is necessary to perform experimental studies taking into account the specific properties of various pipelines, weather conditions, seasons, etc., and to make corresponding technological solutions.

**Acknowledgements.** Yu.M. Andreev and G.V. Lanskii acknowledge the partial support by the Presidium of the Siberian Division, RAS according to Project No. 30.3.2 of Program 30.3.2 ‘Scientific and Scientific and Pedagogical Personnel of Innovation Russia’ (2009–2013) within the framework of State Contract No. 02.740.11.0444, and the support according to Program VII.63.3, Project VII.63.3.1; G.V. Lanskii acknowledges the support according to Resolution No. 465 (21.12.2006).

## References

1. Aleev R.M., Chepurskii V.N., Khoperskii G.G. Patent RF No. 2073816, F17 D5/02, *Izobret.*, No. 5, 225 (1997).
2. Dogan’ A., Osipov M. *Neftegaz. Vertikal*, (7), 3 (2006).
3. Uehara K., Tai H. *Appl. Opt.*, **31**, 809 (1992).
4. Cassidy D.T., Bonnell L.J. *Appl. Opt.*, **27**, 2688 (1988).
5. Cassidy D.T. *Appl. Opt.*, **27** (3), 610 (1988).
6. Petrov K.P., Waltman S., Dlugokensky E.J., Arbore M., Fejer M.M., Tittel F.K., Hollberg L.W. *Appl. Phys. B*, **64**, 567 (1997).
7. Dmitriev V.G., Gurzadyan G.G., Nikogosyan D.N. *Handbook of Nonlinear Optical Crystals* (Berlin: Springer, 1999).
8. Lancaster D.G., Dawes J.M. *Appl. Opt.*, **35**, 4041 (1996).
9. Lee S.W., Zenker T., Chyba T.H. *Proc. 19th Int. Laser Radar Conf. NASA/SP-207671/PT2* (Annapolis, Maryland, 1998) p. 853.
10. Byer R.L., Endermann M. *AIAA J.*, **20**, 395 (1982).
11. Baumgartner R.A., Byer R.L. *Appl. Opt.*, **17**, 3555 (1978).
12. Murray E.R., Van der Laan J.E., Hawley J.G. *Appl. Opt.*, **15**, 3140 (1976).
13. Karapuzikov A.I., Ptashnik I.V., Romanovskii O.A., Kharchenko O.V., Sherstov I.V. *Opt. Atmos. Okean.*, **12**, 364 (1999).
14. Menyuk N., Killinger D.K. *Appl. Opt.*, **26**, 3061 (1987).
15. White K.O., Watkins W.R. *Appl. Opt.*, **14**, 2812 (1975).

16. Kabanov M.V., Andreev Yu.M., Geiko P.P. *Proc. II Int. Conf. Reduce of Methane Mitigation* (Novosibirsk State Techn. Univ., 2000) p. 5.
17. Bertel' I.M., Petukhov V.O., Churakov V.V., Trushin S.A. *Spectros. Lett.*, **16**, 403 (1983).
18. Gorobets V.A., Petukhov V.O., Tochitskii S.Ya., Churakov V.V. *Kvantovaya Elektron.*, **22**, 5 (1995) [*Quantum Electron.*, **25**, 1 (1995)].
19. Andreev Yu.M., Do S.W., Razenkov I.A., Sherstov I.V., Kong H.J. *IR Atmospheric Opt.*, **10**, 119 (1997).
20. Adreev Yu.M., Voevodin V.G., Geiko P.P., Gorobets V.A., Lanskaya O.G., Petukhov V.O., Soldatkin N.P., Tikhomirov A.A. *Lidarnye sistemy i ikh optiko-elektronnye elementy* (Lidar Systems and Their Optoelectronic Elements) (Tomsk: Izd. Inst. Opt. Atmos, SD RAS, 2004).